Chiral-at-Metal BODIPY-Based Iridium(III) Complexes: Synthesis and Luminescence Properties

Marta G. Avello, María C. de La Torre, Andrés Guerrero-martínez, Miguel A. Sierra, Heinz Gornitzka, Catherine Hemmert

Chiral-at-Metal BODIPY-based Iridium(III) Complexes: Synthesis and Luminescent Properties

Marta G. Avello,[a,d] María C. de la Torre,*[,a,d] Andrés Guerrero-Martínez,[b] Miguel A. Sierra,*[c,d] Heinz Gornitzka[e] and Catherine Hemmert[e]

[a]*Instituto de Química Orgánica General. Consejo Superior de Investigaciones Científicas (IQOG-CSIC). Juan de la Cierva 3, 28006 Madrid (Spain).*

[b]*Departamento de Química Física, Facultad de Química Universidad Complutense, 28040 Madrid (Spain).*

[c]*Departamento de Química Orgánica I, Facultad de Química Universidad Complutense, 28040 Madrid (Spain).*

[d]*Centro de Investigación en Química Avanzada (ORFEO-CINQA), Universidad Complutense, 28040-Madrid (Spain).*

[e] *LCC-CNRS, Université de Toulouse, CNRS, UPS, Toulouse, France.*

Abstract.

The synthesis of enantiomerically pure Ir(III) complexes with one or two BODIPY moieties has been achieved through the enantioselective C–H insertion from homochiral triazolium salts, containing a sulfoxide functionality in their structures. These homochiral salts were prepared by the sequential Cu-catalyzed alkyne-azide cycloaddition (CuAAC) of an azide and one alkynyl sulfoxide, followed by a Suzuki coupling in the preformed triazol with a BODIPY containing aryl boronic acid, followed by methylation of the *N3*-triazole nitrogen.

The configuration at the metal in these chiral complexes was established by using a combination of CD and X-ray diffraction techniques. The optical properties of these

complexes were thoroughly studied using spectroscopic (absorption and fluorescence) and computational (TD-DFT and DFT) methods.

The fluorescence of complexes with the BODIPY attached to the sulfoxide moiety (including the two BODIPYs-based complex) was quenched upon introduction of the Ir(III) fragment, most likely due to an *a*-PET mechanism. On the contrary, the fluorescence of Ir(III) complexes with the BODIPY attached to the triazolium ring remains unquenched.

Introduction.

Interest in transition metal complexes having the chromophore 4,4-difluoro-4-bora-3a,4a-diaza-*s*-indacene (BODIPY) systems[1] has increased during the last years. The large number of available structural modifications, due to the presence of the metal compared to the full organic counterparts, allows modulation of the optoelectronic properties of the complexes, as well as their use in different fields ranging from biological labelling to dynamic phototherapy.[2] In return, deactivation of the fluorescence by the presence of the metal is frequently observed. Nevertheless, different and relevant photophysical properties may emerge depending on the mechanism of photodeactivation.[3]

The incorporation of a transition metal center to the BODIPY can be done either by bonding the metal to the peripheries of the BODIPY or directly to the π-conjugated system of this fluorophore. In this regard, the incorporation of a transition metal to a BODIPY through a *N*-heterocyclic carbene ligand (NHC) has been reported. Thus, Plenio described the synthesis of several BODIPY-NHC complexes, including Ru(III), Ir(III), Rh(III), Ir(I), Rh(I), Pd(II) and Au(I) complexes.[4] Additionally, the preparation of Hoveyda-Grubbs catalysts having a BODIPY moiety coordinated to the Ru(I) through the NHC

moiety has been reported and used to follow the metathesis mechanism through fluorescence correlation spectroscopy.[5] Similarly, Ir(I) complexes have been prepared[6] and used for hydrogen detection. Recently, Albrecht has reported the preparation of the first Pd(II) and Ir(II)-1,2,3-triazolylidene complexes and their use in monitoring displacement of ligand reactions.[7] In these cases, the changes in the intensity of the emission of the resulting complexes was an adequate probe to study these processes.

During our work in the synthesis of transition metal complexes having 1,2,3-triazolylidene (MIC) ligands with enantiopure sulfoxide and sulfoxiimine moieties,[8] we have reported the role of the chiral mesoionic carbene ligand (MIC) in defining the catalytic reactivity of their Au(I) derivatives,[9] preparing enantiopure chiral at metal complexes,[10] and enantiopure complexes having chiral-at-metal and chiral planar metallocene moieties.[11] On the other hand our work in push-pull systems containing a Cr(0) and W(0) Fischer metal carbene moiety, **I**, clearly demonstrated that the system geometry is reflected in the deactivation of the fluorescence.[12] Analogously, complexes BODIPY-metal carbene **II**, having remote π-conjugation, allowed to determine the influence of electronic factors in the emission properties of the BODIPY moiety.[13] A similar study was carried out in BODIPYs having remote half-sandwich Ir(III) and Rh(III) moieties, **III** (Figure 1).[14]

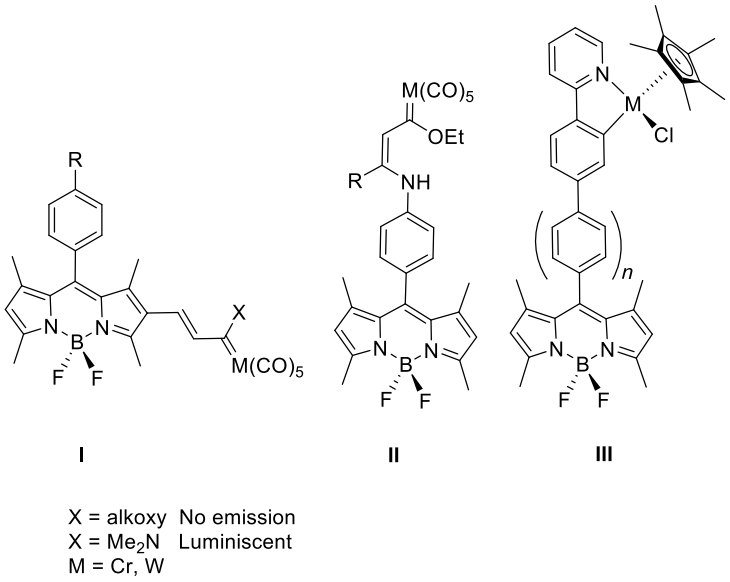

Figure 1. Previously studied Fischer metal carbene BODIPYs push-pull systems (**I, II**) and BODIPYs having remote half-sandwich Ir(III) and Rh(III) (**III)**

Circularly polarized emission (CPL) is rarely observed in systems different from chiral organic molecules[15] and lanthanide complexes.[16] To the best of our knowledge, studies searching for CPL in chiral-at-metal BODIPY containing molecules has not been reported. Our previous work in the field opens an opportunity to watch the possibility of observing CPL in this class of molecules. We now report on the synthesis of homochiral half-sandwich Ir(III) complexes having one or two BODIPY moieties coordinated to the metal by a sulfoxide containing MIC ligand, as well as the study of their chiroptical and photophysical properties. To our knowledge, this is the first time that homochiral transition metal-MIC BODIPYs have been reported.

Results and Discussion.

Access to the three different structural types of 1,2,3-triazole-BODIPY derivatives considered in this study was gained by using enantiopure alkynyl sulfoxides **1** and

anilines **2**. Three differently substituted 1,2,3-triazolyl sulfoxides **3** were obtained by reaction of NfN_3 (nonafluorobutanesulfonyl or nonaflyl azide) and the corresponding aniline to generate "in situ" the azide,[17] and subsequent Cu-catalyzed azide-alkyne cycloaddition in mixtures MeOH/H_2O/Et_2O as solvent, using $CuSO_4.5H_2O$/sodium ascorbate as the catalyst. [8] The yields on compounds **3** were acceptable to good (41-80%) (Scheme 1).

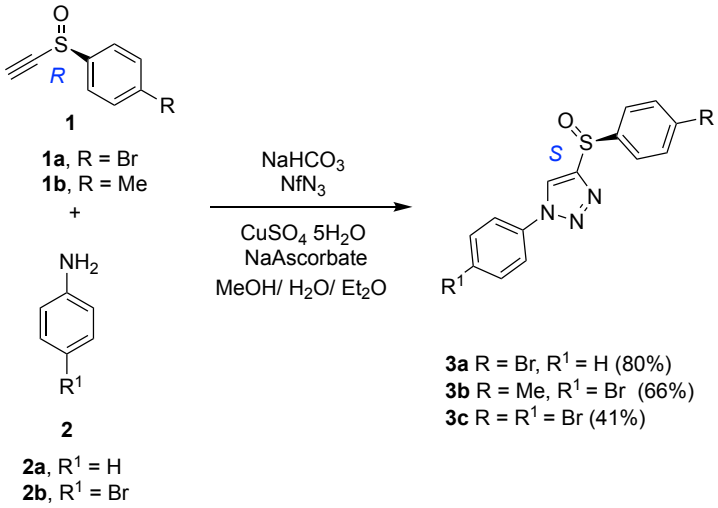

Scheme 1. Synthesis of triazoles **3** by CuAAC between "in situ" generated azides and enantiopure alkynes **1**.

Pinacolyl derivative **4** was prepared following literature procedures[18] and coupled with triazolyl sulfoxide **3a** using $Pd(PPh_3)_4/K_2CO_3$ in a mixture toluene/EtOH/H_2O (4:2:1) as the coupling conditions. Thus, these conditions, which formed the triazolyl-BODIPY **5a** in 94% yield, were used in the preparation of the two additional structural types studied in this work. Thus, coupling of sulfoxide **3b** with BODIPY **4** formed compound **5b** in 79% yield. Compound **5c** having two BODIPY subunits was obtained from 1,2,3-triazole **3c** through a double Suzuki coupling in a 68% yield (Scheme 2). Spectroscopic and

spectrometric data confirm the structures of compounds **3-5**. Compounds **5** were highly colored (orange-green), luminescent products.

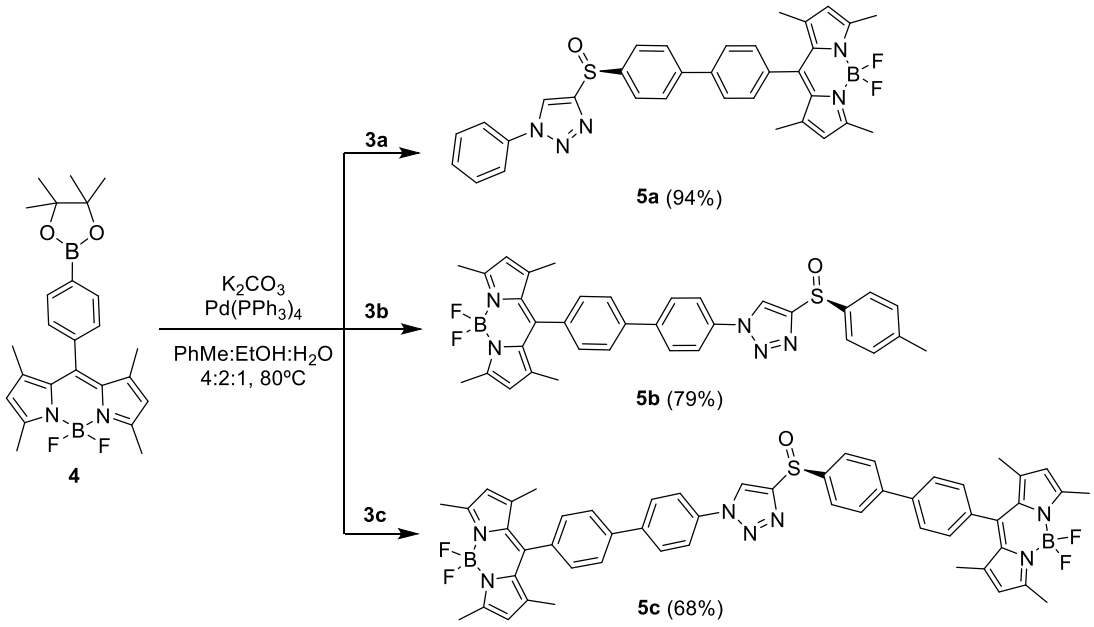

Scheme 2. Suzuki coupling to prepare BODIPY derivatives **5**.

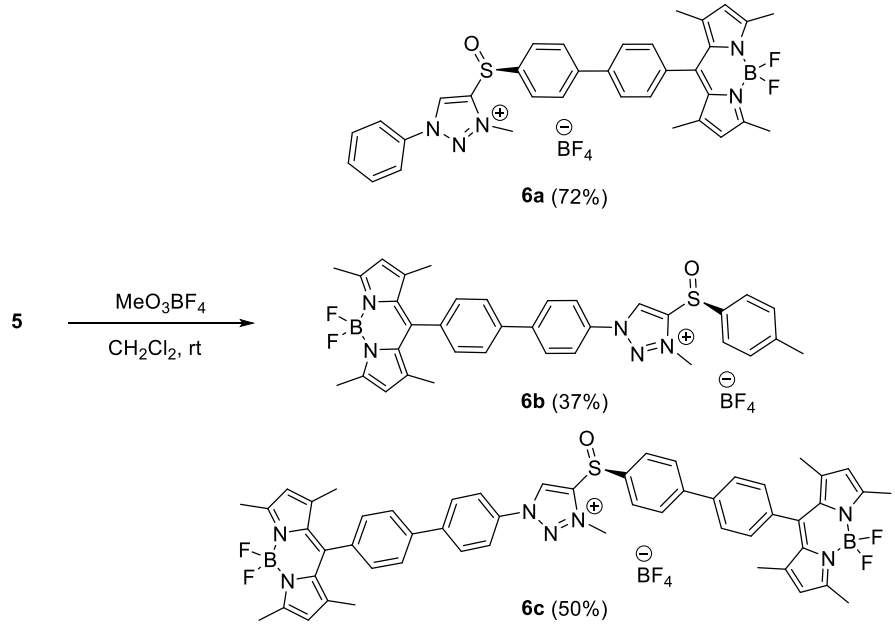

Scheme 3. Methylation of triazoles **5** to obtain the corresponding triazolium salts **6**.

Compounds **5** were methylated with Me_3OBF_4 using the standard conditions to yield the corresponding triazolium salts **6** in acceptable to good yields (37% to 72%) (Scheme 3). Triazolium salts **6** (also strongly colored and fluorescent products) were reacted with

$[IrCl_2Cp^*]_2$ in the presence of Cs_2CO_3. In these conditions a mixture of two products, identified as the desired cyclometallated Ir-complexes **7** and their non-cyclometallated dichloro Ir-precursors, was obtained. The exclusive formation of cyclometallated Ir-complexes **7**, was effected by the sequential treatment of salts **6** with $[IrCl_2Cp^*]_2$ and Cs_2CO_3 until disappearance of the signal corresponding to the H5 of the triazolium ring (8.89-8.94 ppm), followed by treatment of the reaction mixtures with NaOAc, in a one-pot manipulation. In these conditions iridacycles **7a** and **7b** were obtained in 80% and 64% yields, respectively, and bis-iridacycle **7c** in 59% yield (Scheme 4). Compounds **7** having one new chiral-at-metal stereocenter were obtained as single enantiomers. Traces of the corresponding diastereomers (enantiomers at the metallic chiral centers) were not observed in the ^1H NMR spectra of the reaction crude materials.

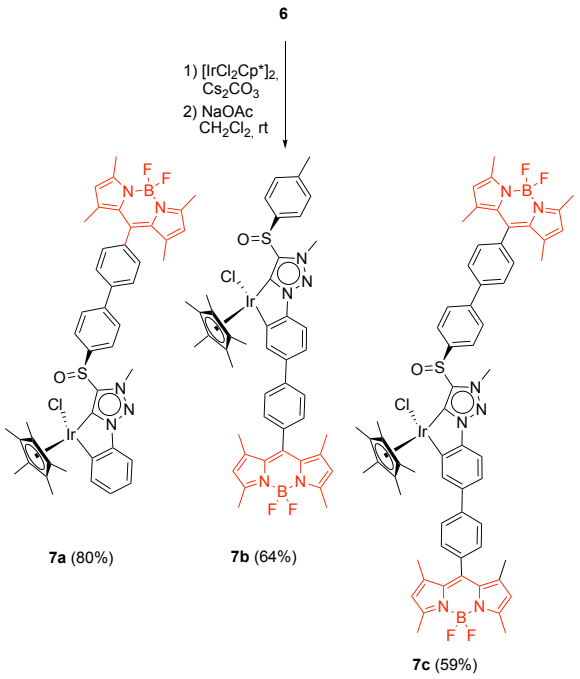

Scheme 4. The synthesis of enantiopure Ir-complexes **7** having BODIPY moieties.

The structure of compounds **7** was determined on spectroscopic grounds. Thus, ^{13}C NMR spectra of complexes **7** show two new quaternary carbon signals assignable to the carbene carbon (156.2 and 156.3 ppm for **7a** and **7b-c**, respectively), and to the

metallated aromatic carbon (144.0 and 145.2 ppm for **7a** and **7b-c**, respectively), which is in accordance with the metallation and the C-H activation reactions. The most characteristic feature of the ^{1}H NMR spectra of iridacycles **7** was the disappearance of the signal corresponding to the H5 of the 1,2,3-triazole ring in the salts **6** (8.89–8.94 ppm), confirming the coordination of the MIC ligand. Finally, a single crystal of complex **7b** was obtained by slow diffusion in a CH_2Cl_2/pentane mixture. The structure and the absolute stereochemistry of complex **7b** was then unambiguously established by X-ray diffraction (Figure 2).

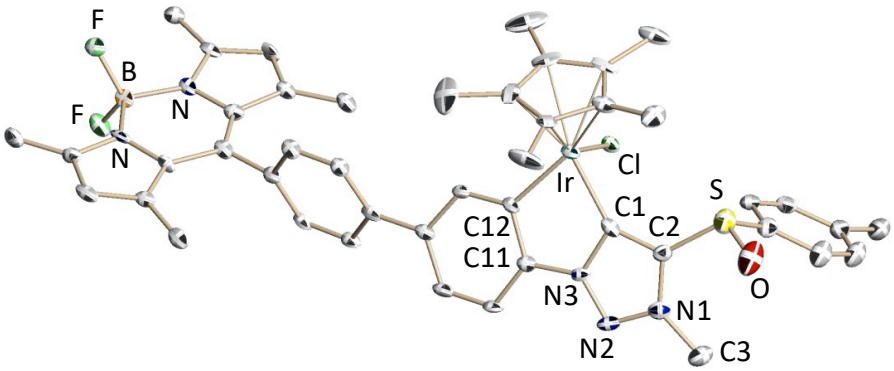

Figure 2. X-ray structure of complex **7b** depicted at a 30% thermal ellipsoid level. Selected bond lengths [Å] and angles [°]: Ir-C1 2.00(2), Ir–C12 2.06(2), Ir-Cl 2.39(1), C1-C2 1.39(2), C2-N1 1.39(2), N1-N2 1.32(2), N2-N3 1.32(2), C1-N3 1.41(2), C2-S 1.75(2), S-O 1.48(2), N1-C3 1.44(2), N3-C11 1.41(2), C1-Ir-Cl 87.3(3), C1-Ir-C12 79.4(4), C12-Ir-Cl 85.4(3).

Complexes **7** were configurationally stable as stablished by recording the ^{1}H NMR spectra of a solution of these complexes after one week in solution. The absolute configuration of complexes **7** was determined by a combination of circular dichroism and X-ray diffraction as previously established by us for similar piano-stool MIC.[10] Figure 3 compiles the CD spectra of compounds **5a**, **6a** and **7a** as representative examples of

the compounds studied in this work (see the SI for the comparative CD spectra of the remaining compounds). Triazole **5a** and triazolium salt **6a** are less absorptive than the iridium complex **7a**. Thus, compounds **5** and **6** always show positive dichroic signals centered at 261.0-285.8 nm and 282.4-292.4 nm respectively, while Ir(III)-complexes have a strong negative Cotton absorption in the range of 253.8 to 290.4 nm. This strong negative Cotton absorption is maintained (287.0 nm) for the Ir(III) complex **7c**.[19] In previous studies,[10] this negative Cotton absorption was assigned to an absolute configuration *R* at the metallic center. Since absolute configuration *R* at the Ir(III) for **7b** has been unambiguously established by X-ray analysis (absolute structure factor x = 0.013(7)), we can conclude that the absolute configuration at the metallic center for complexes **7a** and **7c** may be *R* as well.

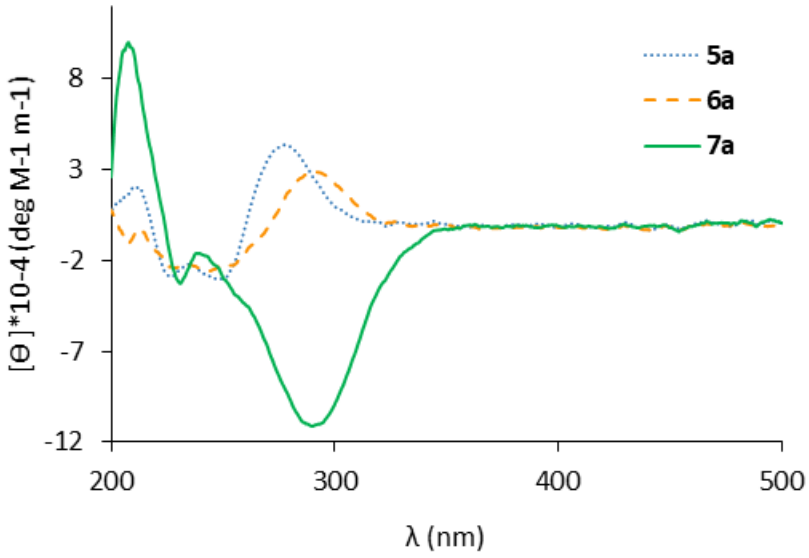

Figure 3. Circular dichroism (CD) spectra of compounds **5a**, **6a**, and **7a** (10 µM solutions in MeCN, T= 25^{o} C).

The photophysical properties of compounds **5, 6** and **7** were studied next. Figure 4 shows the absorption spectra of compounds **5, 6** and **7**, as well as BODIPY **8.** All of them show an absorption pattern analogous to the BODIPYs,[20] with narrow absorption bands

in the region of 467-498 nm composed by two maximum absorptions. The first one and most intense (496-498 nm) is attributable to the vibrational band 0-0 from the electronic transition $S_0 \rightarrow S_1$. The second absorption centered at 467-470 nm is assignable to the vibrational band 0-1 of the same electronic transition. It is worthy to note that the UV/ vis spectra in the 460-500 nm region of non-metallated triazoles **5** and triazolium salts **6** are analogous to the spectra of the cyclometallated compounds **7**. This fact points to a lack of conjugation between the BODIPY and the metallacycle in all derivatives. Further, complex **7c** has an absorption that is double to the equivalent absorptions in complexes **7a** and **7b**, as expected due to the presence of two BODIPY units in its structure.

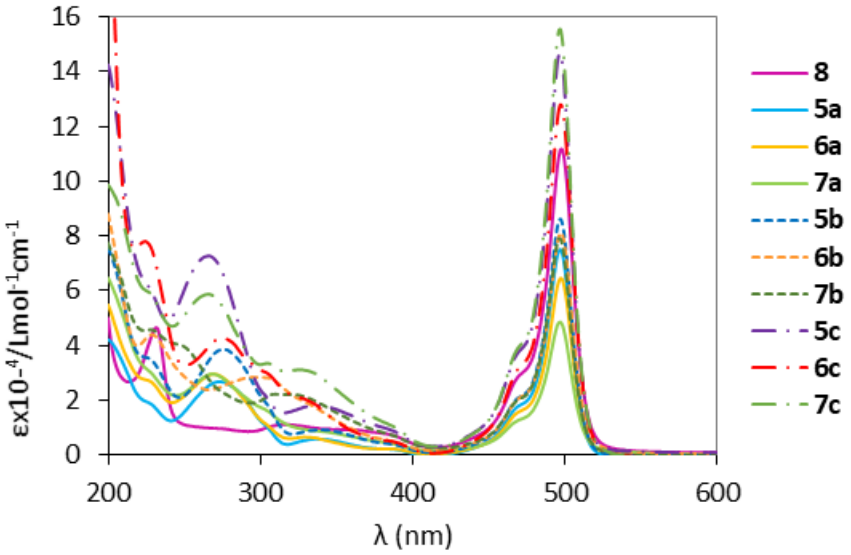

Figure 4. Absorption spectra (MeCN) of compounds **5** and **6** and complexes **7**.

Time-dependent DFT (TD-DFT) calculations were carried out on compounds **5a-b**, **6a-b** and **7a-b** to determine the origin of the vertical transitions associated with the experimental UV/ vis absorptions. The computed transitions nicely agree with the above assignment.

Thus, the band at ca. 500 nm in compounds **5** and **6** is derived from the one electron promotion from the HOMO to the LUMO, which can be regarded as π and $\pi*$ molecular

orbitals fully delocalized in the indacene moiety (see the Figure 5). Analogous orbitals are involved in the HOMO-LUMO vertical transition in the parent BODIPY **8**,[14] which is an additional proof of the exclusive involvement of the indacene moiety in the absorptions around 500 nm. It is noteworthy, that similarly to our previously reported compounds **III**, the contribution from the aryl fragment attached to the BODIPYs **5** and **6** is negligible. Additionally, the band around 500 nm in compounds **7a** and **7b** can be assigned to the HOMO-2 to LUMO and HOMO-1 to LUMO, respectively, which are also $\pi \rightarrow \pi*$ transitions, with both orbitals confined to the BODIPY moiety. Therefore, also in these cases, in which we have a MIC in the coordination sphere of the metal, the metal fragment is a mere spectator. These results clearly confirm that the π-conjugation between the metal centers and the BODIPY fragment is practically negligible. This fact has relevance in the quenching of fluorescence (see below) since a through-skeleton Dexter mechanism for the quenching may be discarded.

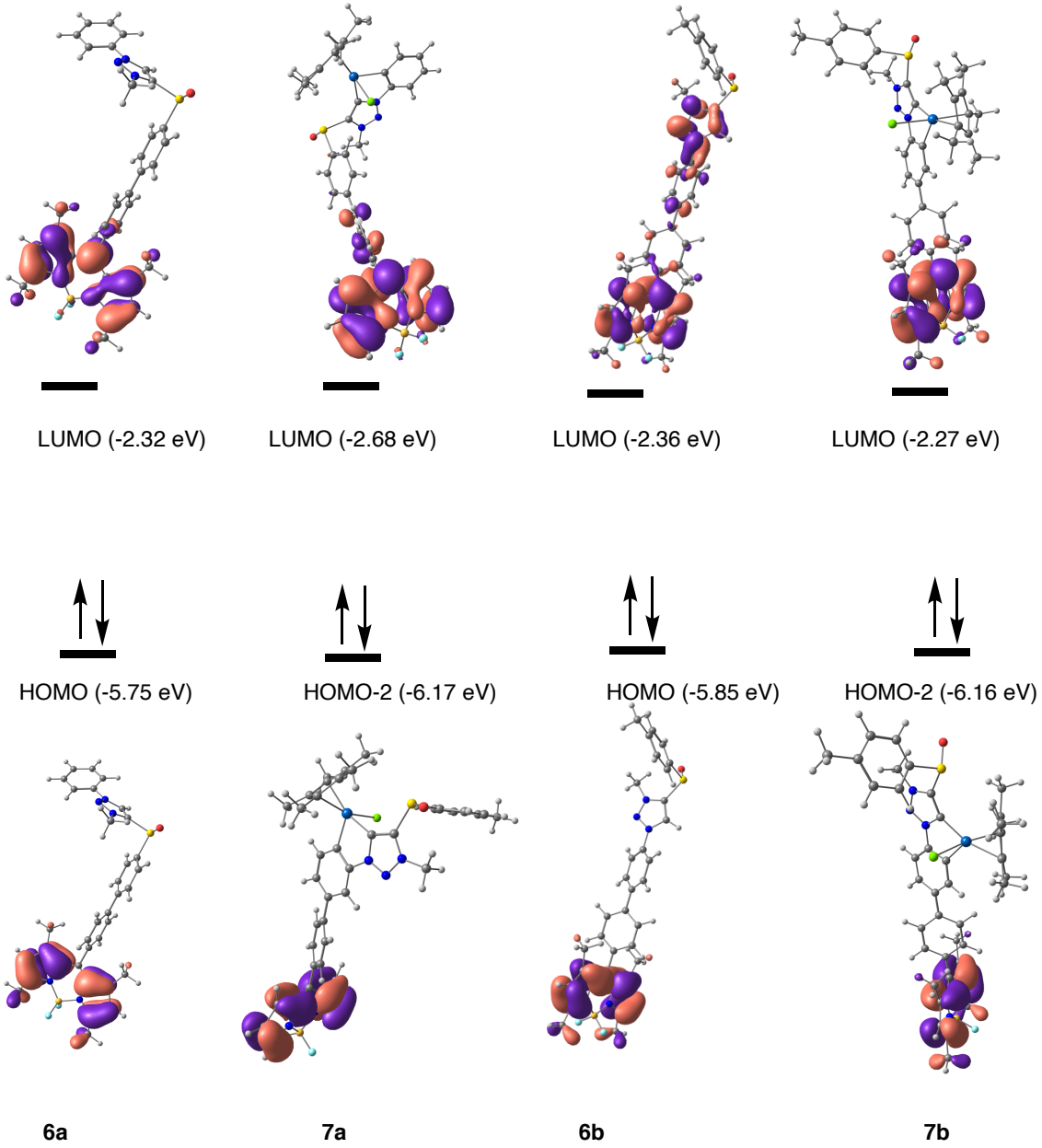

Figure 5. Orbital description of the main absorption transitions on compounds **6** and **7**.

The fluorescence of complexes **5**, **6** and **7** was measured next. Figure 6 compiles the emission spectra of these complexes, together with the emission BODIPY **8** for comparison.

All compounds show narrow emission bands with specular symmetry respect to the absorption bands, a situation that is characteristic of the BODIPYs. The emission bands have maximums at 507-508 nm which corresponds to small Stoke´s shifts (9-10 nm).

Again, the presence of the metal does not significative disturb the profile of the spectra of the BODIPY, except for a slight bathochromic displacement of the triazolium salts **6** respect to triazoles **5** or Ir(III) complexes **7** (Table 1).

Table 1. Photophysical Data of Compounds **5** – **7**.[a]

Compound	λ_{abs} (nm)[b]	ε_{abs}[c]	λ_{em} (nm)[d]	Φ_F[e]
5a	497 (429)[g]	7.48 (0.61)[f]	507	0.69
6a	497 (429)[g]	6.44 (0.70)[f]	508	0.52
7a	497 (420)[g]	4.87 (0.69)[f]	508	0.19
5b	497 (429)[g]	8.64 (0.70)[f]	507	0.7
6b	497 (431)[g]	8.13 (0.70)[f]	508	0.55
7b	497 (429)[g]	7.87 (0.70)[f]	507	0.51
5c	497	14.77	507	0.62
6c	497	12.79	508	0.63
7c	497	15.51	507	0.19

a) All samples were measured at 25 °C in MeCN (concentration of 10^{-5} M, optical density < 0.1). b) Maximum of the UV/ vis spectrum. c) Molar extintion coefficient ε (M^{-1} cm^{-1} x 10^4). d) Maximum of the emission spectrum using λ_{exc} = 450 nm. e) Quantum yields (Φ_F), determined using a 0.1 M solution of fluorescein in NaOH ($\Phi_R = 0.95$) as reference. f) Calculated TD-DFT oscillator strength. g) Calculated TD-DFT excitation energy.

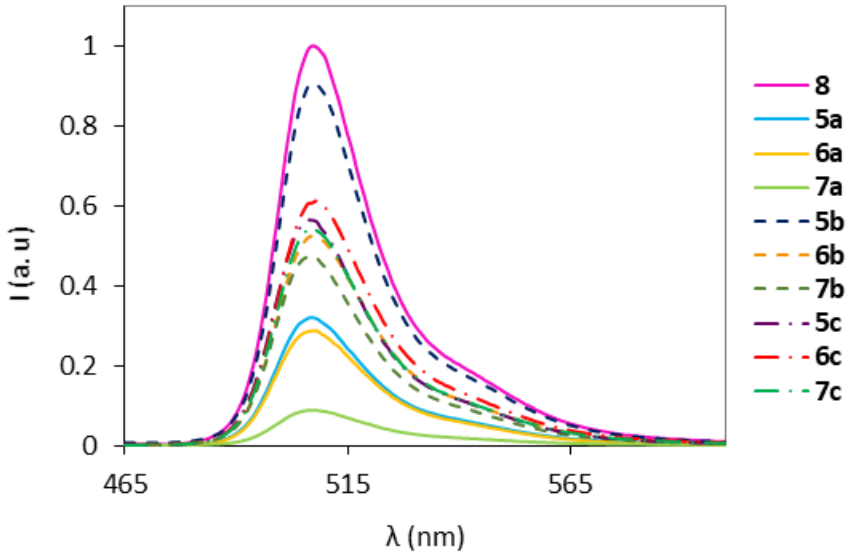

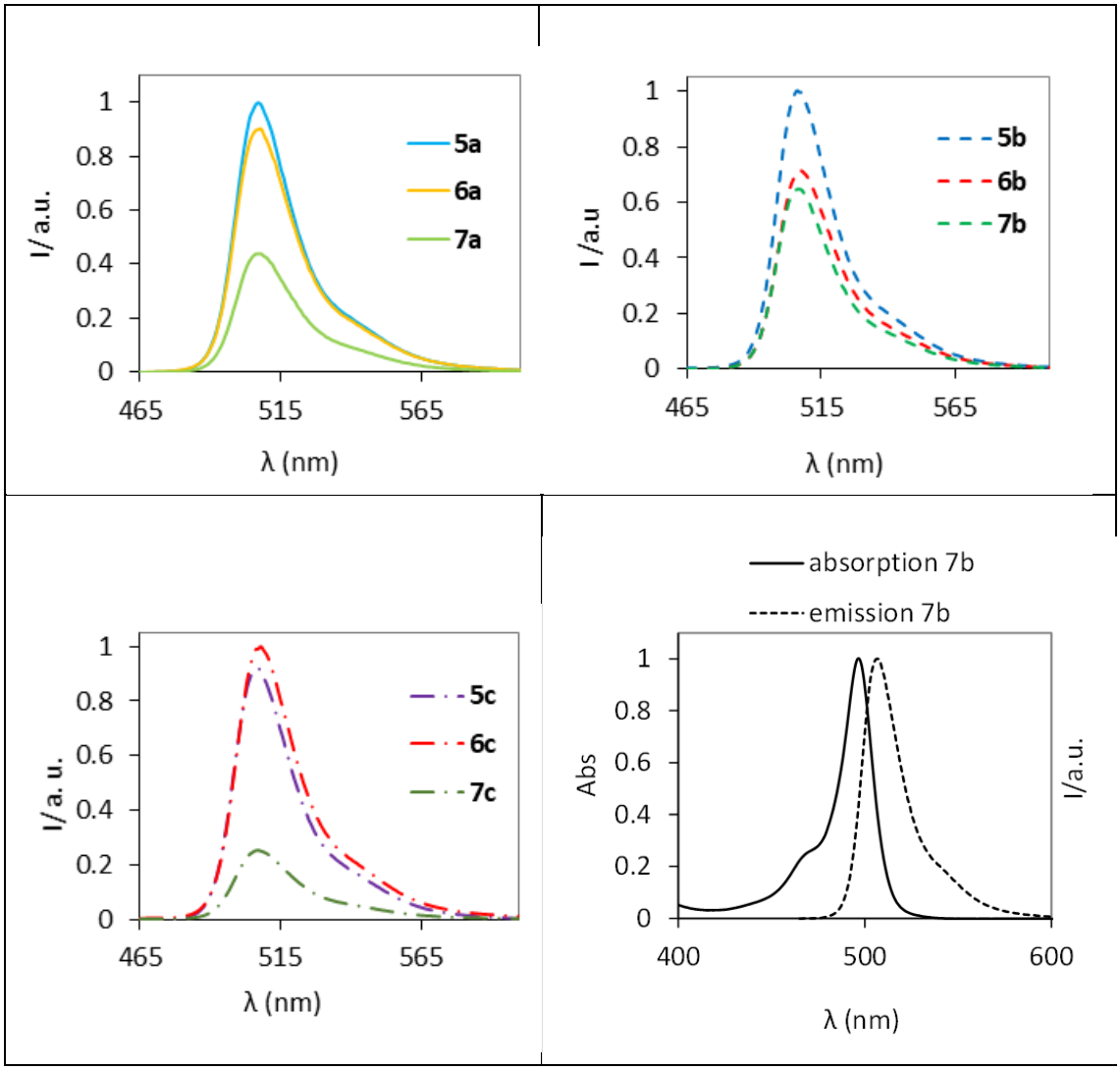

Figure 6. Emission spectra of compounds **5**, **6**, and **7**. The last graphic represents normalized absorption (—) and emission (---) spectra of compound **7b** (bottom right).

The emission spectra of complexes **7** show interesting properties (see Table 1). Thus, as expected due to the presence of the metal, complexes **7a** and **7c** experience a strong quenching of the fluorescence (ϕ = 0.19) respect the corresponding triazoles **5a, 5c** (ϕ = 0.69 and ϕ = 0.55, respectively) and triazolium salts **6a, 6c** (ϕ = 0.52 and ϕ = 0.51, respectively). In clear contrast emission of Ir(III) complex **7b** (ϕ = 0.51) is slightly decreased respect to that of its precursors, namely triazole **5b** and triazolium salt **6b** (ϕ = 0.70 and ϕ = 0.55, respectively). These results show a clear dependence of the

deactivation of the emission process of these complexes with the spatial structure, which may point to a Förster deactivation mechanism.[3]

To understand the quenching mechanism, we registered the UV/ vis spectra of complex **9** (the donor in the Ir(III)-BODIPY donor-acceptor system) and the emission spectra of 4-bromophenyl-BODIPY **8** (the acceptor in the Ir(III)-BODIPY donor-acceptor system) (Figure 7).

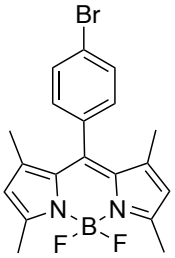

8

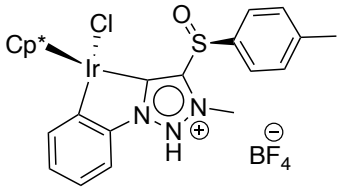

9

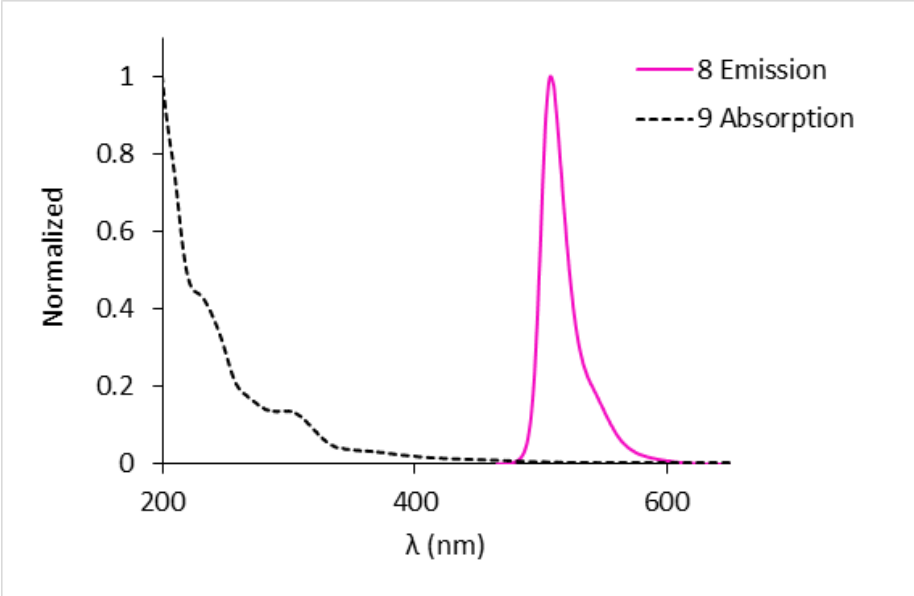

Figure 7. The absorption spectra of complex **9** and the emission spectrum of complex **8** that shows no overlapping between both spectra.

As can be seen in Figure 6, there is no significant overlapping between both absorption and emission spectra which makes the energy transfer either by a through space (Förster) or through skeleton (Dexter) improbable (see above). Therefore, the

quenching of the fluorescence in complexes **7a** and **7c** is likely due to a photoinduced electron transfer mechanism (PET).

To determine the rule of a PET mechanism in the fluorescence deactivation of compounds **7a** and **7c,** we computed the BODIPY fragment **8** and the metal fragments **9** and **10** (compound with an additional phenyl group to determine the influence of the addition of an aromatic group on the emissive properties of the complexes). Figure 8 depicts the HOMO and LUMO of these fragments, where HOMOs of complexes **9** and **10** are higher in energy than the HOMO of the BODIPY **8**. As a consequence, the excitation of the BODIPY core may result in an energetically favorable IMET (intramolecular electron transfer) process from the metallacycle to the BODIPY (ΔE = 0.21 and 0.23 eV, respectively). Based in these results, the BODIPY fragment in complexes **7a** and **7c** may act, upon excitation, as an electron acceptor and the fluorescence may be quenched through an acceptor-excited PET (*a*-PET, $\phi < 0.1$).

However, the extension of the PET mechanism is strongly dependent on the position of the BODIPY moiety. According to the model in Figure 8, the fluorescence of complex **7b** would be quenched by the effect of the metal atom (as in complex **7a**). Moreover, the fluorescence complex **7c**, with similar structural features to complexes **7a** and **7b** is quenched. This fact points to the role of the moiety similar to **7a** as the fluorescence quenching element, overcoming the role of the moiety similar to **7b** in maintaining the emissive properties of the compound. To this moment, the reasons behind this strong differential behavior in closely related complexes remain elusive.

Finally, all attempts to detect CPL in complexes **7** either with lineal horizontal/vertical or circular polarization, as well as with circular excitation and detection meet with no avail.

Conclusions.

The synthesis of enantiomerically pure Ir(III) complexes having one or two BODIPY moieties in their structures has been achieved through the enantioselective C–H insertion from homochiral triazolium salts **6**. These homochiral salts are easily available through the Cu-catalyzed alkyne-azide cycloaddition (CuAAC) of an *in situ* generated azide (from the corresponding amine and nonaflyl azide) and alkynyl sulfoxide **1**. The BODIPY moiety was incorporated into the preformed triazol by a Suzuky coupling using BODIPY aryl boronic acid **4**. Homochiral salts **6a-c** were obtained by methylation with Me_3OBF_4. Homochiral salt **7c** with two BODIPY moieties was accessed by a double Suzuki coupling using boronic acid **4** which incorporated both BODIPY moieties and triazole **2c** followed by methylation.

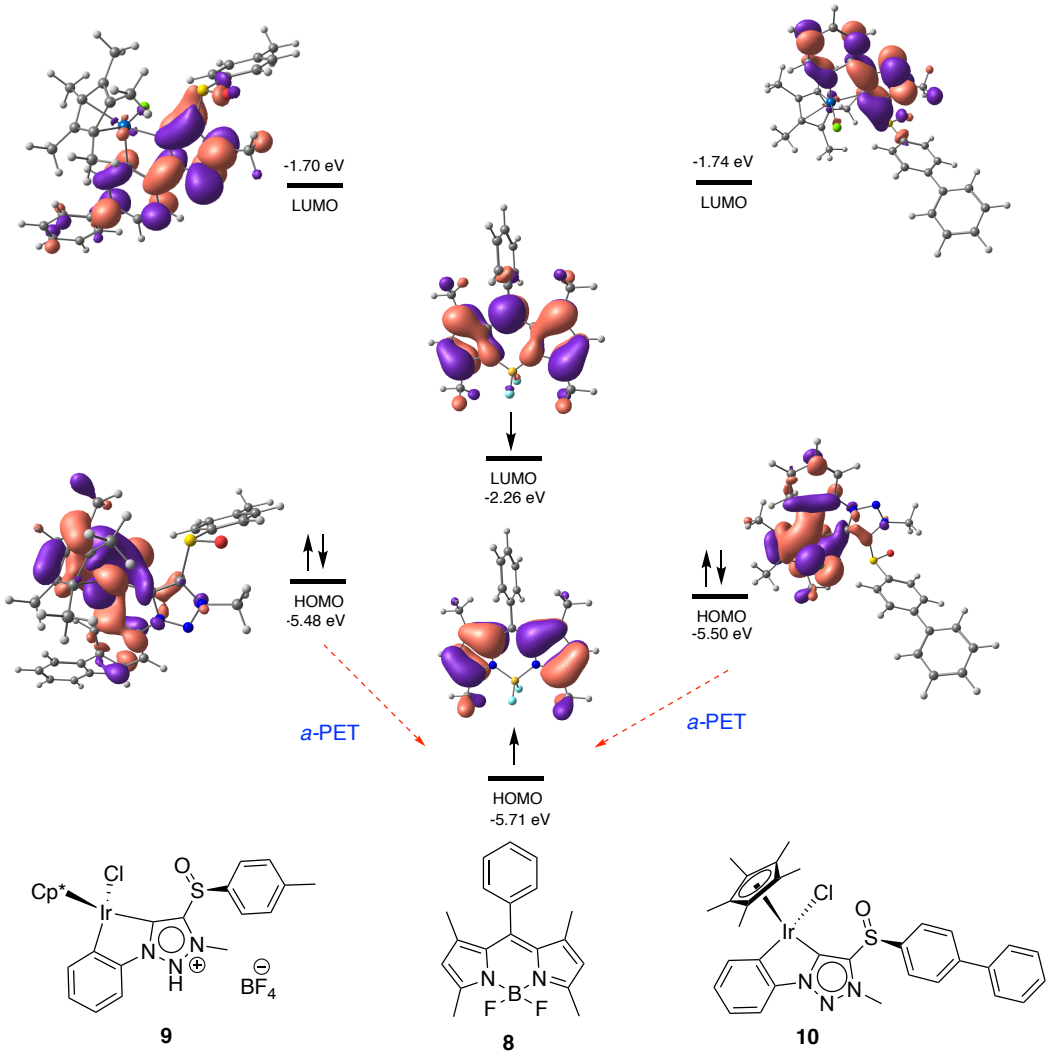

Figure 8. Orbital distribution and HOMO-LUMO energies of BODIPY **8**, complex **9**, and complex **10**.

Complexes **7a-c** were obtained as single enantiomers. The absolute configuration at the metal was established by using a combination of CD and X-ray diffraction. The optical properties of these complexes were thoroughly studied. Thus, complexes **7a** and **7c** show a significative quenching of fluorescence respect to their precursors, namely triazoles **5a** and **5c**, as well as the corresponding triazolium salts **6a** and **6c** that were strongly fluorescent. Meanwhile, the fluorescence of complex **7b** is only slightly decreased respect to the fluorescent precursors **5b** and **6b**. Based on extensive TD-DFT and DFT computations, the quenching of fluorescence in complexes **7a** and **7c** upon

introduction of the Ir(III) fragment could be explained through a *a*-PET mechanism. However, the persistence of the fluorescence in complex **7b** is still not well understood. The fluorescence of complex **7b** is striking, not only due to the close resemblance between complexes **7a** and **7b**, but due to the fact that the fluorescence of complex **7c** having the structural features of complexes **7a** (strong quenching of fluorescence) and **7b** (emissive) is quenched, like in complex **7a**. To the best of our knowledge complex **7b** is the single example of a fluorescent homochiral Ir(III) complex.[21]

Efforts to prepare other homochiral fluorescent metal-BODIPY complexes in search of CPL properties are now underway in our laboratories.

Experimental Section.

General. Unless noted otherwise, all manipulations were carried out under argon atmosphere using standard Schlenk techniques. CH_3CN, THF and DCM were dried by passage through solvent purification columns containing activated alumina. Other solvents were HPLC grade and were used without purification. All reagents were obtained from commercial sources and used without additional purification, unless noted otherwise. Flash column chromatography was performed using silica gel (Merck, n° 9385, 230-400 mesh). ^1H and ^{13}C NMR spectra were recorded at 300, 400 or 500 MHz (^1H NMR) and at 75, 100 or 126 MHz (^{13}C NMR) using $CDCl_3$ and CD_3CN as solvents with the residual solvent signal as internal reference ($CDCl_3$, 7.26 and 77.2 ppm; CD_3CN, 1.94 and 118.69 ppm). The following abbreviations are used to describe peak patterns when appropriate: s (singlet), d (doublet), t (triplet), q (quadruplet), m (multiplet), and br s (broad singlet). High-resolution mass spectrometry (HRMS) by the ESI technique was performed with an Agilent 6500 accurate mass apparatus with a Q-TOF analyser. IR spectra were recorded on a Perkin-Elmer 681 spectrophotometer. Optical rotations were measured on a Jasco P-2000 polarimeter using a sodium lamp. Circular Dichroism curves were obtained on a Jasco J-815 Spectropolarimeter. Melting points were determined on a Koffler block. UV/ vis absorption spectra were registered using a UVICON XL spectrophotometer (Bio-Tex Instruments). Fluorescence spectra were

recorded using an AMINCO Bowman Series 2 spectrofluorometer, with 1.0 nm bandwidth for emission and excitation.

Alkynes **1a** and **1b**[22], triazole **3a**[10] and BODIPY **4** [23] were prepared according to previously described procedures.

1,2,3-Triazole (3b). A solution of 4-bromoaniline (0.70 g, 4.07 mmol) in H_2O (8.0 mL)/ MeOH (12.0 mL) was treated with $NaHCO_3$ (1.37 g, 16.28 mmol), NfN_3 (1.99 g, 6.10 mmol) in Et_2O (20.0 mL) and $CuSO_4.5H_2O$ (0.10 g, 0.401 mmol). After 6 h of stirring, alkyne **1b** (0.735 g, 4.48 mmol) and sodium *L*-ascorbate (1.21 mg, 6.11 mmol) were added. The mixture was stirred for another 18 h. The residue was concentrated under reduced pressure, dissolved in CH_2Cl_2, washed with a $NaHCO_3$ saturated aqueous solution, dried and concentrated under *vacuum*. After flash chromatography (Hexanes/EtOAC/CH_2Cl_2 5:2:3, v/v/v), pure triazol **3b** (0.95 g, 66%) was obtained as a light brown solid.

^{1}H NMR (400 MHz, $CDCl_3$): δ 8.29 (s, 1H, N_3C=CH), 7.70 (d, *J* = 8.0 Hz, 2H, Ar *p*-tol), 7.64 (d, *J* = 8.9 Hz, 2H, Ar *p*-Br-C_6H_4), 7.58 (d, *J* = 8.9 Hz, 2H, Ar *p*-Br-C_6H_4), 7.33 (d, *J* = 7.9 Hz, 2H, Ar *p*-tol), 2.40 (s, 3H, CH_3 *p*-tol).

^{13}C NMR (101 MHz, $CDCl_3$): δ 154.5 (C, N_3**C**=CH), 142.5 (C, *p*-tol), 139.9 (C, *p*-tol), 135.4 (C, *p*-Br-C_6H_4), 133.2 (2CH, Ar *p*-Br-C_6H_4), 130.3 (2CH, Ar *p*-tol), 124.9 (2CH, Ar *p*-tol), 123.4 (C, *p*-Br-C_6H_4), 122.2 (2CH, Ar *p*-Br-C_6H_4), 122.0 (CH, N_3C=**C**H), 21.6 (CH_3, *p*-tol).

IR (KBr): $\nu_{máx}$ 1900, 1739, 1593, 1498, 1236, 1032, 819 cm^{-1}**.**

$[\alpha]^{25}_D$ = + 230.77 (*c* 0.73 $CHCl_3$).

HRMS (ESI) *m/z* calcd for $C_{15}H_{12}BrN_3OS$: 363.9937 $[M+H]^+$; found 363.9946.

M.p: 175-177 °C.

BODIPY-1,2,3-triazole (5b). A mixture of triazole **3b** (299 mg, 0.83 mmol) and BODIPY **4** (340 mg, 0.76 mmol) in the presence of K_2CO_3 (418 mg, 3.02 mmol) and $Pd(PPh_3)_4$ (53 mg, 0.045 mmol) in toluene (18.0 mL), EtOH (9.0 mL) and H_2O (14.5 mL) was stirred at 90 ˚C overnight. The mixture was filtered through a pad of Celite, diluted with CH_2Cl_2 and washed with H_2O and brine. The organic phase was dried over anhydrous Na_2SO_4,

filtered and solvents removed under *vacuum*. After flash chromatography (hexanes/EtOAc, 3:2), pure compound **5b** (363 mg, 79%) was obtained as a deep orange solid.

^{1}H NMR (400 MHz, $CDCl_3$): δ 8.33 (s, 1H, N_3C=CH), 7.82 (s, 4H, Ar), 7.76 (m, 4H, Ar), 7.40 (d, *J* = 6.7 Hz, 2H, Ar *p*-tol), 7.36 (d, *J* = 8.2 Hz, 2H, Ar *p*-tol), 6.00 (s, 2H, BODIPY), 2.57 (s, 6H, $2CH_3$ BODIPY), 2.42 (s, 3H, CH_3 *p*-tol), 1.44 (s, 6H, $2CH_3$ BODIPY).

^{13}C NMR (101 MHz, $CDCl_3$): δ 155.8 (2C, Ar BODIPY), 154.4 (C, N_3**C**=CH), 143.1 (2C, Ar BODIPY), 142.5 (C, Ar *p*-tol), 141.4 (C, Ar), 141.0 (C, Ar), 140.0 (C, Ar), 139.9 (C, Ar), 136.0 (C, Ar), 135.1 (C, Ar), 131.5 (2C, Ar BODIPY), 130.4 (2CH, Ar *p*-tol), 129.0 (2CH, Ar *p*-tol), 128.6 (2CH, Ar), 127.8 (2CH, Ar), 124.9 (2CH, Ar), 121.9 (CH, N_3C=**C**H), 121.5 (2CH, Ar BODIPY), 121.1 (2CH, Ar), 21.6 (CH_3, *p*-tol), 14.7 ($4CH_3$, BODIPY).

IR (KBr): $\nu_{máx}$ 1543, 1511, 1470, 1306, 1196, 1157, 982, 823, 810 cm^{-1}.

$[\alpha]^{25}_{D}$ = + 173.88 (*c* 1.01, $CHCl_3$).

HRMS (ESI) *m/z* calcd for $C_{34}H_{30}BF_2N_5OS$: 606.2311 $[M+H]^+$; found 606.2329.

M.p: Decomposes.

BODIPY-1,2,3-triazolium salt (6b). Triazole **5b** (202 mg, 0.33 mmol) was treated with Meerwein salt (73 mg, 0.50 mmol) in CH_2Cl_2 (20.0 mL) at rt until completion of the reaction (TLC analysis). The reaction was quenched with a few drops of methanol and the solvents were removed under *vacuum*. The residue was solved in the minimum amount of CH_2Cl_2 and precipitated with Et_2O. Solvents were poured off and the solid washed with Et_2O and dried under *vacuum*. After flash chromatography (MeOH/CH_2Cl_2 5% v), pure **6b** (85 mg, 37%) was obtained as a reddish orange solid.

^{1}H NMR (500 MHz, CD_3CN): δ 8.90 (s, 1H, N_3C=CH), 8.02 (d, J = 8.4 Hz, 2H, Ar), 7.92 (d, J = 8.5 Hz, 2H, Ar), 7.89 (d, J = 8.1 Hz, 2H, Ar), 7.84 (d, J = 8.0 Hz, 2H, Ar *p*-tol), 7.55 (d, J = 8.0 Hz, 2H, Ar *p*-tol), 7.50 (d, J = 8.1 Hz, 2H, Ar), 6.11 (s, 2H, BODIPY), 4.39 (s, 3H, N-CH_3), 2.50 (s, 6H, $2CH_3$ BODIPY), 2.48 (s, 3H, CH_3 *p*-tol), 1.45 (s, 6H, $2CH_3$ BODIPY).

^{13}C NMR (126 MHz, CD_3CN): δ 156.6 (2C, Ar BODIPY), 148.2 (C, N_3**C**=CH), 146.1 (C, Ar *p*-tol), 144.8 (C, Ar), 144.5 (2C, Ar BODIPY), 142.6 (C, Ar), 140.2 (C, Ar), 136.9 (C, Ar *p*-tol), 136.1 (C, Ar), 135.0 (C, Ar), 132.1 (2C, Ar BODIPY), 132.0 (2CH, Ar *p*-tol), 130.1 (CH, N_3C=**C**H), 130.0 (2CH, Ar), 129.9 (2CH, Ar), 129.0 (2CH, Ar), 126.9 (2CH, Ar *p*-tol), 123.4 (2CH, Ar), 122.4 (2CH, Ar BODIPY), 40.8 (CH_3, N-**C**H_3), 21.7 (CH_3, *p*-tol), 14.8 ($2CH_3$, BODIPY), 14.7 ($2CH_3$, BODIPY).

IR (KBr): $\nu_{máx}$ 1544, 1511, 1307, 1197, 1158, 1085, 1061, 983, 824 cm^{-1}.

$[\alpha]^{25}_{D}$ = + 114.37 (*c* 0.08, $CHCl_3$).

HRMS (ESI) *m/z* calcd for $C_{35}H_{33}BF_2N_5OS$: 620.2468 $[M\text{-}BF_4]^+$; found 620.2469.

M.p: Decomposses.

BODIPY-Iridacycle (7a). To a solution of triazolium salt **6a** (60 mg, 0.09 mmol) in CH_2Cl_2 (8.0 mL), $[IrCl_2Cp^*]_2$ (65 mg, 0.08 mmol) and Cs_2CO_3 (68 mg, 0.21 mmol) were added. The reaction mixture was stirred at rt until completion of the reaction (^{1}H NMR analysis). The mixture was filtered through a pad of Celite. Addition of NaOAc (19 mg, 0.23 mmol) and stirring for another 24 h yielded, after flash chromatography (MeOH/CH_2Cl_2 3% v) pure **7a** (87 mg, 80%) as a deep orange solid.

^{1}H NMR (400 MHz, $CDCl_3$): δ 8.09 (d, *J* = 8.3 Hz, 2H, Ar), 7.92 (d, *J* = 6.4 Hz, 1H, Ar), 7.81 (d, *J* = 8.5 Hz, 2H, Ar), 7.70 (d, *J* = 8.0 Hz, 2H, Ar), 7.60 (dd, *J* = 7.8, 1.4 Hz, 1H, Ar), 7.37 (d, *J* = 7.9 Hz, 2H, Ar), 7.18 (td, *J* = 7.4, 1.4 Hz, 1H, Ar), 7.03 (td, *J* = 7.5, 1.3 Hz, 1H, Ar), 5.98 (s, 2H, BODIPY), 4.06 (s, 3H, N-CH_3), 2.56 (s, 6H, 2CH_3 BODIPY), 1.91 (s, 15H, 5CH_3 Cp*), 1.41 (s, 6H, 2CH_3 BODIPY).

^{13}C NMR (101 MHz, $CDCl_3$): δ 156.2 (C, N_3C=**C**Ir), 155.8 (2C, Ar BODIPY), 144.6 (C, Ar), 144.0 (C, Ar), 143.5 (C, N_3**C**=CIr), 143.1 (3C, C Ar + 2C Ar BODIPY), 141.1 (C, Ar), 140.3 (C, Ar), 139.8 (C, Ar), 136.9 (CH, Ar), 135.1 (C, Ar), 131.5 (2C, Ar BODIPY), 129.6 (CH, Ar), 129.0 (2CH, Ar), 128.6 (2CH, Ar), 127.9 (2CH, Ar), 126.1 (2CH, Ar), 122.7 (CH, Ar), 121.5 (2CH, Ar BODIPY), 114.3 (CH, Ar), 91.6 (5C, Cp*), 38.2 (CH_3, N-**C**H_3), 14.8 (2CH_3, BODIPY), 14.7 (2CH_3, BODIPY), 9.9 (5C, CH_3 Cp*).

IR (KBr): $\nu_{máx}$ 2917, 1544, 1511, 1470, 1410, 1307, 1195, 1157, 1085, 1051, 983, 823 cm^{-1}.

$[\alpha]^{25}_{D}$ = − 367.67 (*c* 0.1, $CHCl_3$).

HRMS (ESI) *m/z* calcd for $C_{44}H_{44}BF_2IrN_5OS$: 932.2960 $[M+H]^+$; found 932.2968.

M.p: Decomposes.

Computational details. All calculations were performed at the DFT level using the M06 functional[24] with an ultrafine integration grid[25] in conjunction with the D3 dispersion correction suggested by Grimme[26] 40 as implemented in Gaussian 16.[27] S, Cl and Ir atoms were described using the scalar-relativistic Stuttgart-Dresden SDD

pseudopotential[28] and its associated double-ζ basis set complemented with a set of f-polarization functions.[29] The 6-31G** basis set was used for the H, C, N, F and O atoms. [30] All structures of the reactants, intermediates, transition states, and products were fully optimized in dichloromethane solvent (ε = 8.93) using the SMD continuum model.[31] Calculations of absorption spectra were accomplished by using the time-dependent density functional theory (TD-DFT)[32] method at the same level. All energies collected in the text are Gibbs energies in dichloromethane at 298 K.

Crystallographic details. All data were obtained using an oil-coated shock-cooled crystal of **7b** on a Bruker-AXS APEX II diffractometer with MoKa radiation (λ = 0.71073 Å) at 100(2) K. The crystal structure was solved by direct methods[33] and all non-hydrogen atoms were refined anisotropically using the least-squares method on F^2 [34]. The absolute configuration has been refined using the Flack parameter x[35]. **Crystal data of 7b:** $C_{45}H_{46}BClF_2IrN_5OS$, MW 981.39 g/mol, orthorhombic, $P2_12_12_1$, a = 9.925(1) Å, b = 20.070(2) Å, c = 21.726(2) Å, V = 4327.4(4) $Å^3$, 28987 reflections have been measured, 8755 independent reflections, Rint = 0.0893, 525 parameters have been refined using 20 restraints, R1 (I>2σ) = 0.0548, wR2 (I>2σ) = 0.0969, R1 (all data) = 0.0776, wR2 (all data) = 0.1032, absolute structure parameter x = 0.013(7), largest diff. peak = 1.488 $eÅ^{-3}$. CCDC-2005906 contains the additional crystallographic data. These data can be obtained free of charge from the Cambridge Crystallographic Data Centre via www.ccdc.cam.ac.uk/data_request/cif.

Supporting Information.

Characterization and Experimental Procedures for compounds **5c**, **6a**, **6c**, **7b**, **7c.** Circular Dichroism spectra of compounds **5-7b** and **5-7c**. Copies of NMR spectra of new compounds, crystallographic details and Cartesian Coordinates (PDF).

Conflict of Interest

The authors declare no conflict of interest.

ACKNOWLEDGMENTS

Support for this work under grants CTQ2016-77555-C2-1-R to M.A.S., CTQ2016-77555-C2-2-R to M.C.T. and CTQ2016-81797-REDC Programa Redes Consolider from the AEI (Spain) is gratefully acknowledged. MAS thanks the Fundación Ramón Areces for a grant from the XVII Concurso Nacional de Ayudas a la Investigación en Ciencias de la Vida y de la Materia (CIVP18A3938). Dr. Marta García-Avello thanks the AEI for one FPI predoctoral grant.

References.

[1] Selected reviews: (a) A. Loudet, K. Burgess, *Chem. Rev.* **2007**, *107*, 4891–4932. (b) G. Ulrich, R. Ziessel, A. Harriman *Angew.Chem. Int. Ed.* **2008**, *47*, 1184– 1201. (c) N. Boens, V. Leen, W. Dehaen, *Chem. Soc. Rev.* **2012**, *41*, 1130–1172. (d) J. Zhao, K. Xu, W. Yang, Z. Wang, F. Zhong, *Chem. Soc. Rev.* **2015**, *44*, 8904–8939.

[2] Selected recent references on the different applications of metallo-BODIPYs: (a) B. Bertrand, K. Passador, C. Goze, F. Denat, E. Bodio, M. Salmain, *Coord. Chem. Rev.* **2018**, *358*, 108–124. (b) G. Gupta, P. Kumari, J. Y. Ryu, J. Lee, S. M. Mobin, C. Y. Lee, *Inorg. Chem***. 2019**, *58*, 8587-8595 (c) J. Zhou, Y. Zhang, G. Yu, M. R. Crawley, C. R. P. Fulong, A. E. Friedman, S. Sengupta, J. Sun, Q. Li, F. Huang, T.R. Cook, *J. Am. Chem. Soc.* **2018**, *140*, 7730 -7736. (d) M. Zhang, S. Li, X. Yan, Z. Zhou, M. L. Saha, Y.-C. Wang, P. J. Stang, *J. Am. Chem. Soc.* **2017**, *139*, 5067–5074. (e) C. Y. Lee, O. K. Farha, B. J. Hong, A. A. Sarjeant, S. T. Nguyen, J. T. Hupp, *J. Am. Chem. Soc.* **2011**, *133*, 15858-15861. (f) Y. Jeong, J. Yoon, *Inorg. Chim. Acta* 2012, *381*, 2-14. (g) D. Wang, R. Malmberg, I. Pernik, S. K. K. Prasad, M. Roemer, K. Venkatesan, T. W. Schmidt, S. T. Keaveney, B. A. Messerle, *Chem. Sci.,*

2020, *11*, 6256-6267. (h) M. A. Filatov, *Org. Biomol. Chem,* **2020**, *18*, 10-27. (i) V. N. Nemykin, T. S. Blesener, C. J. Ziegler, *Macroheterocycles* **2017**, *10*, 9–26. (j) G. Ghosh, K. L. Colón, A. Fuller, T. Sainuddin, E. Bradner, J. McCain, S. M. A. Monro, H. Yin, M. W. Hetu, C. G. Cameron and S. A. McFarland, *Inorg. Chem.,* **2018**, *57*, 7694–7712. (k) R. P. Paitandi, V. Sharma, V. D. Singh, B. K. Dwivedi, S. M. Mobin, D. S. Pandey, *Dalton Trans.* **2018**, *47*, 17500-17514.

[3] For deactivation mechanisms see: Joseph R. Lakowicz, *Principles of Fluorescence Spectroscopy*, Springer, **2006**.

[4] P. Kos, H. Plenio, *Chem. Eur. J.* **2015**, *21*, 1088–1095.

[5]J. Godoy, V. García-López, L. Y. Wang, S. Rondeau-Gagné, S. Link, A. A. Martí, J. M. Tour, *Tetrahedron* **2015**, *71*, 5965–5972.

[6] P. Kos, H. Plenio, *Angew. Chem. Int. Ed.* **2015**, *54*, 13293–13296.

[7] M. Navarro, S. Wang, H. Müller-Bunz, G. Redmond, P. Farràs, M. Albrecht, *Organometallics* **2017**, *36*, 1469–1478.

[8] M. A. Sierra, M. C. De La Torre, *ACS Omega* **2019**, *4*, 12983–12994.

[9] M. Frutos, M. G. Avello, A. Viso, R. Fernández de la Pradilla, M. C. De La Torre, M. A. Sierra, H. Gornitzka, C. Hemmert, *Org. Lett.* **2016**, *18*, 3570–3573.

[10] M. G. Avello, M. Frutos, M. C. delaTorre, A. Viso, M. Velado, R. F. de la Pradilla, M. A. Sierra, H. Gornitzka, C. Hemmert, *Chem. Eur. J.* **2017**, *23*, 14523–14531.

[11] M. G. Avello, M. C. la Torre, M. A. Sierra, H. Gornitzka, C. Hemmert, *Chem. Eur. J.* **2019**, *25*, 13344–13353.

[12] G. M. Chu, A. Guerrero-Martinez, I. Fernandez, M. A. Sierra, *Chem. Eur. J.* **2014**, *20*, 1367–1375.

[13] G. M. Chu, A. Guerrero-Martínez, C. R. De Arellano, I. Fernández, M. A. Sierra, *Inorg. Chem.* **2016**, *55*, 2737–2747.

[14] G. M. Chu, I. Fernández, A. Guerrero-Martínez, C. Ramírez De Arellano, M. A. Sierra, *Eur. J. Inorg. Chem.* **2016**, *2016*, 844–852.

[15] Recent reviews: (a) J.-L. Ma, Q. Peng, C.-H. Zhao *Chem. Eur. J.* **2019**, 25,15441 –15454. (b) H. Tanaka, Y. Inoue, T. Mori, *ChemPhotoChem* **2018**, *2*, 386–402.

[16] Selected reviews: (a) F. Zinna, L. Di Bari, *Chirality* **2015**, *27*, 1-13. (b) R. Carr, N. H. Evans, D. Parker, *Chem. Soc. Rev.* **2012,** *41,* 7673-7686. (c) Y. Kitagawa, M. Tsurui, Y. Hasegawa, *ACS Omega* **2020**, *5*, 3786-3791

[17] J. R. Suárez, B. Trastoy, M. E. Pérez-Ojeda, R. Marín-Barrios, J. L. Chiara, *Adv. Synth. Catal.* **2010**, *352*, 2515–2520.

[18] J. Zhai, T. Pan, J. Zhu, Y. Xu, J. Chen, Y. Xie, Y Qin, *Anal. Chem.* **2012**, *84*, 10214–10220.

[19] Compounds **7** were configurationally stable in solution as determined by ^{1}H-NMR.

[20] (a) H. Lu, J. MacK, Y. Yang, Z. Shen, *Chem. Soc. Rev.* **2014**, *43*, 4778–4823. (b) W. Qin, M. Baruah, A. Stefan, M. Van Der Auweraer, N. Boens, *ChemPhysChem* **2005**, *6*, 2343–2351. (c) M, Kollmannsberger, K. Rurack, U. Resch-Genger, J. Daub, *J. Phys. Chem. A* **1998**, *102*, 10211–10220.

[21] It can be though that complexes **6** have a participation of Dexter and Förster mechanisms, which are important in complexes **6a** and **6c** and less important for complex **6b**. However, additional data to support this hypothesis will be required.

[22] H. Kosugi, M. Kitaoka, K. Tagami, A. Takahashi, H. Uda, *J. Org. Chem.* **1987**, *52*, 1078–1082.

[23] J. Zhai, T. Pan, J. Zhu, Y. Xu, J. Chen, Y. Xie, Y. Qin, *Anal. Chem.* **2012**, *84*, 10214–10220.

[24] (a) Y. Zhao, D. G. Truhlar, *Theor. Chem. Acc.* **2008**, *120*, 215–241. (b) Y. Zhao, D. G. Truhlar, *Acc. Chem. Res.* **2008**, *41*, 157–167. (c) Y. Zhao, D. G. Truhlar, *Chem. Phys. Lett.* **2011**, *502*, 1–13.

[25] S. E. Wheeler, K. N. Houk, *J. Chem. Theory Comput.* **2010**, *6*, 395-404.

[26] S. Grimme, J. Antony, S. Ehrlich, H. A. Krieg, *J. Chem. Phys.* **2010**, *132*, 154104.

[27] Gaussian 16. Revision C.01, M. J. Frisch, G. W. Trucks, H. B. Schlegel, G. E. Scuseria, M. A. Robb, J. R. Cheeseman, G. Scalmani, V. Barone, G. A. Petersson, H. Nakatsuji, X. Li, M. Caricato, A. V. Marenich, J. Bloino, B. G. Janesko, R. Gomperts, B. Mennucci, H. P. Hratchian, J. V. Ortiz, A. F. Izmaylov, J. L. Sonnenberg, D. Williams-Young, F. Ding, F. Lipparini, F. Egidi, J. Goings, B. Peng, A. Petrone, T. Henderson, D. Ranasinghe, V. G. Zakrzewski, J. Gao, N. Rega, G. Zheng, W. Liang, M. Hada, M. Ehara, K. Toyota, R. Fukuda, J. Hasegawa, M. Ishida, T. Nakajima, Y. Honda, O. Kitao, H. Nakai, T. Vreven, K. Throssell, J. A. Montgomery, Jr., J. E. Peralta, F. Ogliaro, M. J. Bearpark, J. J. Heyd, E. N. Brothers, K. N. Kudin, V. N. Staroverov, T. A. Keith, R. Kobayashi, J. Normand, K. Raghavachari, A. P. Rendell, J. C. Burant, S. S. Iyengar, J. Tomasi, M. Cossi, J. M. Millam, M. Klene, C. Adamo, R. Cammi, J. W. Ochterski, R. L. Martin, K. Morokuma, O. Farkas, J. B. Foresman, and D. J. Fox, Gaussian, Inc., Wallingford CT, 2016.

[28] D. Andrae, U. Häuβermann, M. Dolg, H. Stoll, H Preuβ, *Theor. Chim. Acta* **1990**, *77,* 123-141.

[29] A. W. Ehlers, M. Böhme, S. Dapprich, A. Gobbi, A. Höllwarth, V. Jonas, K. F. Köhler, R. Stegmann, A. Veldkamp, G. Frenking, *Chem. Phys. Lett.* **1993**, *208*, 111-114.

[30] (a) W. J. Hehre, R. Ditchfield, J. A. Pople, *J. Chem. Phys.* **1972**, *56*, 2257. (b) M. M. Francl, W. J. Pietro, W. J. Hehre, J. S. Binkley, M. S. Gordon, D. J. DeFrees, J. A. Pople, *Chem. Phys.* **1982**, *77*, 3654-3665.

[31] A. V. Marenich, C. J. Cramer, D. G. Truhlar, *J. Phys. Chem. B* **2009**, *113*, 6378-6396.

[32] (a) M. E. Casida, Recent Developments and Applications of Modern Density Functional Theory, Vol. 4, Elsevier, Amsterdam, 1996; (b) M. E. Casida, D. P. Chong, Recent Advances in Density Functional Methods, Vol. 1, World Scientific, Singapore, 1995, p. 155.

[33] G. M. Sheldrick, *Acta Cryst*. **2008**, *A64*, 112–122.

[34] G. M. Sheldrick, *Acta Cryst*. **2015**, *C71*, 3-8.

[35] S. Parsons, H.D. Flack, T. Wagner, *Acta Cryst*. **2013**, *B69*, 249–259.

TOC:

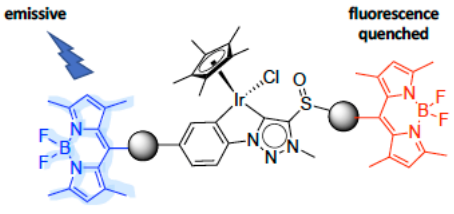

Text for the TOC:

Chiral at metal, enantiomerically pure Ir(III) complexes having one or two BODIPY moieties have been prepared for the first time, using a enantioselective C–H activation reaction. The stereochemistry of these complexes was assigned using CD-X-ray techniques. Emissive properties of these compounds depend on the position of the

BODIPY moiety. Fluorescence is quenched when BODIPY is attached to the substituent in the sulfoxide and maintained if attached to the substituent in the triazole ring.